Biomolecules and Biomedicine
ISSN: 2831-0896 (Print) | ISSN: 2831-090X (Online)
Journal Impact Factor® (2022): 3.4
CiteScore® (2022): 5.3
www.biomolbiomed.com | blog.biomolbiomed.com

RESEARCH ARTICLE

TRANSLATIONAL AND CLINICAL RESEARCH

Role and mechanism of KIAA1429 in regulating cellular ferroptosis and radioresistance in colorectal cancer

Hao Chen[1], Peipei Zhu[1], Dan Zhu[1], Juan Jin[2], Qianni Yang[3]*, and Xiaodong Han[4]*

[1]Department of Gastroenterology, Dazhou Hospital of Integrated Traditional Chinese and Western Medicine, Dazhou, China.

[2]Department of Oncology, Linyi Third People's Hospital, Linyi, China.

[3]Department of Gastroenterology, Shanxi Cancer Hospital, Taiyuan, China.

[4]Gynecological Radiotherapy Ward, Shanxi Cancer Hospital, Taiyuan, China.

***Corresponding authors:** Qianni Yang; Email: yangqianni07@163.com; Xiaodong Han; Email: fx58811aoak8643@163.com.

DOI: https://doi.org/10.17305/bb.2024.10313

Submitted: 26 January 2024/ **Accepted:** 11 April 2024/ **Published online:** 05 June 2024

Conflicts of interest: Authors declare no conflicts of interest.

Funding: Authors received no specific funding for this work.

ABSTRACT

Colorectal cancer (CRC) is one of the most common non-cutaneous malignancies, causing significant mortality and a substantial burden. This study aims to explore the role of KIAA1429 (also known as vir-like m6A methyltransferase associated [VIRMA]) protein in the radioresistance of CRC. CRC cells and a radioresistant cell line were cultured, and KIAA1429 expression was detected. After the down-regulation of KIAA1429, its effect on the radioresistance and ferroptosis of cancer cells was analyzed. The role of ferroptosis in radioresistance was verified. The binding relationship among long non-coding RNA endogenous Bornavirus-like nucleoprotein 3, pseudogene (LncRNA EBLN3P), microRNA (miR)-153-3p, and KIAA1429 was analyzed. KIAA1429 and LncRNA EBLN3P were highly expressed in CRC, while miR-153-3p was poorly expressed. KIAA1429 and LncRNA EBLN3P were further increased/decreased in the radioresistant cells. KIAA1429 knockdown decreased the survival rate of the radioresistant cell line after X-ray irradiation and increased gamma H2A histone family member X (γ-H2AX), ferroptosis, and oxidative stress. A ferroptosis inhibitor alleviated the inhibitory effect of KIAA1429 knockdown on radioresistance. KIAA1429-mediated m6A modification up-regulated LncRNA EBLN3P, and LncRNA EBLN3P increased KIAA1429 by competitively binding to miR-153-3p. miR-153-3p silencing or LncRNA EBLN3P overexpression attenuated the promotion of ferroptosis and the inhibition of radioresistance induced by KIAA1429 knockdown. Overall, KIAA1429-mediated m6A modification up-regulated LncRNA EBLN3P expression, and LncRNA EBLN3P increased KIAA1429 expression by competitively binding to miR-153-3p, thus reducing ferroptosis and increasing the radioresistance of CRC.

Keywords: Colorectal cancer; ferroptosis; radioresistance; KIAA1429; LncRNA EBLN3P; miR-153-3p; γ-H2AX; m6A.

INTRODUCTION

Colorectal cancer (CRC) ranks as the third most commonly diagnosed cancer and the second most common cause of cancer-associated death around the world [1]. In 2023, about 153,020 individuals were diagnosed with CRC and 52,550 died from it, including 19,550 cases and 3750 deaths in individuals younger than 50 years [2]. It is estimated that the number of new cases of CRC will increase by 63%, to 3.2 million per year by 2040, while the mortality rate will increase by 73 percent, to 1.6 million per year [3]. Various genes and the interaction of many pathways have been implicated in the oncogenesis of CRC, but the complex mechanism remains incompletely understood [4]. The development of CRC is a multi-step process triggered by benign polyps, which may evolve into cancer through the interaction between environmental and genetic factors [5]. Additionally, abnormal cell proliferation, cell differentiation, resistance to apoptosis, invasion of adjacent structures by colorectal tumor cells, and distant metastasis are associated with CRC carcinogenesis, whose mechanisms of action are complex and remain incompletely understood [3]. Primary treatment methods for CRC include surgery, chemotherapy, radiotherapy, immunotherapy, and targeted therapy, and yet they all have their shortcomings [6]. Therefore, CRC is a global public health challenge in terms of morbidity, mortality, and availability of healthcare services [7].

N6-methyladenosine (m6A) is the most common, abundant, and conserved internal transcriptional modification, and m6A modification is installed by the m6A methyltransferases [8]. KIAA1429 (vir-like m6A methyltransferase associate) is a major m6A methyltransferase that plays important biological and pharmacological roles in human diseases [9]. KIAA1429 is related to various biological behaviors, such as benign/poorly differentiated tumor pathways and tumor metastasis pathways [10]. In particular, KIAA1429 has been found to regulate aerobic glycolysis in CRC in an HK2-dependent manner [11]. In addition to glycolysis, KIAA1429 can modulate ferroptosis of oral squamous cell carcinoma cells and ferroptosis may

represent a promising target in tumor resistance to therapy, radiotherapy included [12, 13]. However, the role of KIAA1429 in the radiotherapy resistance of CRC remains unknown.

Long non-coding RNAs (LncRNAs) are >200-nt-long RNA transcripts that do not encode protein and are functional units themselves [14]. Previous research has shown that lncRNAs play a crucial role in CRC [15]. LncRNA endogenous bornavirus-like nucleoprotein (EBLN3P), for instance, stimulates CRC progression by regulating U2AF Homology Motif Kinase 1 (UHMK1) expression via sponging miR-323a-3p [16], reflecting lncRNAs participation in CRC progression by coordinating with microRNAs (miRNAs), a group of small non-coding RNAs that post-transcriptionally control expression of genes by targeting mRNAs [17, 18]. LncRNA ZNFX1 antisense RNA 1-mediated miR-153-3p has been implicated in CRC cell growth and metastasis [19]. Nonetheless, the interaction between lncRNA EBLN3P and miR-153-3p has not been investigated. Given that m6A regulators can affect CRC development by regulating lncRNAs and lncRNAs can modulate m6A modification by completing with m6A regulators [20], this paper aims to explore the functions of KIAA1429, lncRNA EBLN3P, and miR-153-3p in CRC from the perspective of radioresistance, thus providing some promising therapeutic targets for CRC patients.

MATERIALS AND METHODS

Cell culture

Normal intestinal epithelial cell line (NCM460) and CRC cell lines (HCT116, SW620, LoVo) were procured from ATCC and cultured in DMEM containing 10% fetal bovine serum and 1% antibiotics at 37°C with 5% CO_2 and 95% air.

Establishment of radioresistant cell lines

Radioresistant cells were established according to the previous description [21]. When HCT116 and SW620 cells reached 50% confluence, they were irradiated at 4 Gy. Then, these

cells were repeatedly irradiated with 4 Gy until the total radiation dose reached 40 Gy. The obtained radioresistant cell lines were named HCT116R and SW620R.

Cell transfection

EBLN3P overexpression vector (EBLN3P) and empty vector (NC) were obtained from Shanghai GenePharma. KIAA1429 siRNAs (si-KIAA1429-1, KIAA1429-2, and KIAA1429-3) or EBLN3P siRNAs (si-EBLN3P EBLN3P-1, si-EBLN3P-2) or negative control (si-NC), miR-153-3p mimics (mimics-153), miR-153-3p inhibitor (inhi-153), and corresponding controls (mimics-NC, inhi-NC) were purchased from GenePharma. The above plasmids or siRNAs were transfected into cells by Lipofectamine 2000 (Invitrogen, Carlsbad, CA, USA). The transfection was verified by reverse transcription-quantitative polymerase chain reaction (RT-qPCR) or Western blot 48 h later.

Treatment of ferroptosis inhibitors

The cells were pre-treated with 5 μM Ferrostatin-1 (SML0583, Sigma-Aldrich, Missouri, USA) or DMSO (Solarbio, Beijing, China) for 24 h before irradiation.

Irradiation

Different doses of irradiation were performed at room temperature using a 6-megavolt-X-raylinear accelerator (Varian, EDGE, USA). The radiation conditions were as follows: treatment field of 40 × 40 cm, source-skin distance of 100 cm, and radiation dose rate of 5 Gy/min.

Cell Counting Kit-8 (CCK-8) method

Cell viability was assessed by CCK-8 assay. These cells (2000 cells/well) were seeded in 96-well plates. At 24, 48, and 72 h after irradiation, 10 μL of CCK-8 solution (02432300, Cellor Lab, China) was added for further 3-h incubation. The optical density (OD) values were measured at 450 nm using a microplate reader (Multiskan™ FC, 51119180ET, Thermo Fisher Scientific, USA). In addition, a blank background group containing only DMEM was set to

eliminate the OD value of the medium. The calculation formula for the cell proliferation rate is: cell proliferation rate (%) = (OD treatment group−OD Blank)/(OD control group−OD Blank) × 100%.

Colony formation assay

Cell survival after radiation was defined as the ability of cells to maintain clonogenic capacity and subsequently form colonies. Cells were counted and seeded in 6-well plates at 500 cells/well. Cells were exposed to the indicated doses of radiation and incubated at 37°C for 12-14 d. Colonies were stained with crystal violet and manually counted, and colonies of ≥50 cells were recorded.

Immunofluorescence

Cells were subjected to 4% paraformaldehyde fixation and 1% TritonX-100 permeabilization. After sealing, they were incubated with γ-H2AX antibody (A700-053, Thermo Fisher Scientific, USA) for 2 h or IgG antibody (ab150079, Abcam) for 1 h, and then stained with DAPI (Thermo Fisher Scientific) for 5 min at 37°C. Finally, cell observation was performed using a fluorescence microscope (Olympus, Japan).

Fe^{2+}, reactive oxygen species (ROS), and glutathione (GSH) assays

Fe^{2+} levels in cells were detected using the Iron Ion Colorimetric Assay Kit (E1042, Applygen Technologies, Beijing, China).

ROS levels were measured by adding 20 μM cell permeabilization probe 2′,7′-dichlorodihydrofluorescein diacetate (DCFH-DA; Sigma). After incubation for 30 min, the intensity of the fluorescence produced at 485 nm excitation wavelength and 530 nm emission wavelength was measured using a fluorescence spectrometer.

For GSH detection, a commercially available GSH assay kit (A006-1-1, built in Nanjing, China) was used. The absorbance at 420 nm was captured to calculate the GSH content.

Quantification of m6A

m6A RNA methylation was detected using the m6A RNA Methylation Assay Kit (ab185912, Abcam). The absorbance at 450 nm was measured and the percentage of m6A to total RNA (400 ng) of each group was calculated.

Methylated RNA immunoprecipitation (MeRIP)

MeRIP assays for gene m6A modifications were performed using the Magna MeRIP Kit (CR203146, Millipore, MA, USA). Briefly, cells were washed twice with ice-cold PBS and then collected by centrifugation (1500 g, 4°C, 5 min). After removal of the supernatant, cells were mixed with 100 μL of RIP lysis buffer and incubated on ice for 5 min. Anti-m6A antibody (ab208577, Abcam) was coated on magnetic beads, washed twice with RIP washing buffer, and resuspended (900 μL of RIP immunoprecipitation buffer + 100 μL of cell lysate). After overnight incubation at 4°C, the beads were washed and extracted for RNA enrichment analysis by RT-qPCR.

RNA stability assay

Cells were seeded in 6-well plates and treated with actinomycin D (5 μg/mL, Sigma-Aldrich, St. Louis, MO, USA) for 0 h, 3 h, and 6 h. Total RNA was extracted for RT-qPCR.

Nuclear/cytoplasmic fractionation

Cellular localization was performed using the PARIS kit (Invitrogen). Briefly, the nuclear and cytoplasmic fractions were separated and finally calculated by RT-qPCR. U6 snRNA and GAPDH were used as positive controls for the nuclear and cytoplasmic fractions, respectively.

RNA immunoprecipitation (RIP)

RIP analysis was performed using the Magna RIP kit (Millipore, Billerica, MA, USA). Cells were lysed with lysis buffer containing protease inhibitors and ribonuclease inhibitors for 30 min on ice and centrifuged (25,000 g, 4°C, 5 min). The supernatant was then used as input (positive control). IgG (ab172730, Abcam), Ago2 (ab186733, Abcam), and protein A/G-beads

were added to the supernatant. After centrifugation at 4°C, the samples were spun and incubated overnight. Protein A/G-bead precipitates were washed three times. Relative RNA in the precipitate after isolation and purification was verified by RT-qPCR.

Dual-luciferase assay

The binding relationships between the ceRNA networks were predicted by the Targetscan database (https://www.targetscan.org/vert_71/) [22] and the Starbase database (https://rnasysu.com/encori/index.php) [23]. ENBL3P and KIAA1429 mRNA 3'-UTR sequences containing miR-153-3p complementary sites were cloned into pGL3-control luciferase reporter vectors (Promega, Madison, WI, USA), named ENBL3P-WT or KIAA1429-WT. The mutation sites were named ENBL3P-MUT or KIAA1429-MUT. WT or MUT sequence was cotransfected into cells with miR-153-3p mimics or mimics-NC. Twenty-four hours after transfection, luciferase activity was assessed by the luciferase reporter system (Promega).

RT-qPCR

Total RNA was extracted from cells with the TRIzol reagent (Invitrogen) and then reverse transcribed into cDNA at 42˚C for 30 min using a PrimeScript™ RT kit (Takara). qPCR was performed using iTaq™ Universal SYBR®-Green Supermix (Bio-Rad) on an ABI 7500 instrument (Applied Biosystems). GAPDH or U6 [24] was used as an internal reference. Relative expression was calculated by the 2-ΔΔCt method [25]. Primers are shown in Table 1.

Western blot

Proteins were collected from cells using RIPA buffer (Beyotime). Then, protein concentration was determined by the BCA method (Beyotime). Subsequently, proteins (40 μg/lane) were separated by 10% SDS-PAGE (Beyotime) and transferred to PVDF membranes (EMD Millipore). The PVDF membranes were blocked with 5% skim milk powder for 1.5 h at room temperature. The membranes were then incubated with primary antibodies KIAA1429 (1:1000,

ab271136, Abcam), SLC7A11 (1:1000, ab307601, Abcam), GPX4 (1:1000, ab125066, Abcam), ACSL4 (1:10,000, ab155282, Abcam), and GAPDH (1:2500, ab9485, Abcam) overnight at 4°C. The next day, membranes were washed three times with PBS containing 0.2% Tween-20 (PBST) and treated with secondary antibody (1:2000, ab205718, Abcam) for 1.5 h at room temperature. Afterwards, the immunoreactive bands were again washed with PBST. Finally, the signals were monitored and visualized using an enhanced chemiluminescence assay (EMD Millipore) and an Odyssey infrared imaging system (LI-COR Biosciences). GAPDH was used as an internal reference. ImageJ software (version 1.52r; NIH) was utilized to semi-quantify the intensity of the bands.

Statistical analysis

All data were statistically analyzed and graphed using SPSS 21.0 statistical software (IBM, NY, USA) and GraphPad Prism 8.0 software (GraphPad Software Inc., San Diego, CA, USA). Normality and chi-square tests were first performed to confirm normal distribution and homogeneity of variance. The t-test was utilized for data comparison between two groups for measurement data; one-way or two-way ANOVA was used for data comparison among multiple groups, and Tukey's test was applied for post-hoc tests. P value was obtained from two-sided tests, with $p < 0.05$ indicating statistical significance and $p < 0.01$ indicating extreme significance.

RESULTS

KIAA1429 increases radioresistance in CRC cells

KIAA1429 is highly expressed in CRC, but its effect on cancer cell radioresistance is unclear. We examined KIAA1429 expression and the results showed that KIAA1429 expression was increased in CRC cells ($P < 0.01$, Figure 1A-B). We selected 2 cell lines with relatively low KIAA1429 expression to establish radioresistant cells HCT116R and SW620R. Compared with parental cells, the radioresistant cells exhibited a higher proliferation rate ($P < 0.01$, Figure

1C) and higher expression of KIAA1429 ($P < 0.01$, Figure 1A-B). To verify the role of KIAA1429 on CRC cell radioresistance, we downregulated KIAA1429 expression in cells ($P < 0.01$, Figure 1D-E), The si-KIAA1429-1 and si-KIAA1429-2 with better intervention efficiency were selected for the subsequent experiments. Parental cells with a survival rate of close to 50% were treated with 4 Gy. Cells with low expression of KIAA1429 had a slowed proliferation rate ($P < 0.01$, Figure 1F) and a reduced number of clonal cells ($P < 0.01$, Figure 1G). The positivity of γ-H2AX was notably increased after the knockdown of KIAA1429 ($P < 0.01$, Figure 1H). The above results suggest that KIAA1429 promotes radioresistance in CRC cells.

KIAA1429 knockdown promotes ferroptosis in CRC cells

Numerous studies have reported that ferroptosis is associated with radioresistance in cancer cells. We also explored the effect of KIAA1429 on ferroptosis. After KIAA1429 knockdown, 4 Gy radiation resulted in increased levels of Fe^{2+} in HCT116R and SW620R cells ($P < 0.01$, Figure 2A). In addition, the expression of ferroptosis-associated protein ACSL4 was enhanced and SLC7A11 and GPX4 decreased after KIAA1429 knockdown ($P < 0.01$, Figure 2B-C). Downregulation of KIAA1429 resulted in increased ROS levels and decreased GSH content ($P < 0.01$, Figure 2D-E). Taken together, KIAA1429 knockdown promoted ferroptosis in CRC cells.

KIAA1429 increases radioresistance in CRC cells by inhibiting ferroptosis

The use of Fer-1, a ferroptosis inhibitor, was intended to validate the role of ferroptosis changes in the modulation of radioresistance by KIAA1429. As shown in Figure 3A-B, Fer-1 treatment with 4 Gy radiation led to decreased levels of Fe^{2+} and ACSL4 and increased levels of SLC7A11 and GPX4 in HCT116R cells ($P < 0.01$). And the addition of Fer-1 led to decreased ROS levels and increased GSH content ($P < 0.01$, Figure 3C-D). After decreasing ferroptosis, the proliferation rate of cells increased ($P < 0.01$, Figure 3E), the number of clonal cells

increased ($P < 0.01$, Figure 3F), and the positivity of γ-H2AX was markedly reduced ($P < 0.01$, Figure 3G). Briefly, KIAA1429 increased the radioresistance of CRC cells by inhibiting ferroptosis.

KIAA1429-mediated m6A modification upregulates LncRNA EBLN3P expression

KIAA1429 is the major m6A methyltransferase and EBLN3P expression is increased in CRC [16]. Our results showed the same and showed higher expression in radioresistant cells ($P < 0.01$, Figure 4A). Through the m6A online tool (http://www.cuilab.cn/sramp/), a sequence-based m6A modification site predictor, we found m6A sites on the EBLN3P sequence (Figure 4B). We speculated that EBLN3P is downstream of KIAA1429. m6A quantitative analysis showed that the m6A enrichment level was downregulated in KIAA1429 low-expressing cells ($P < 0.01$, Figure 4C). Further analysis revealed that m6A levels were upregulated in EBLN3P RNA but downregulated after KIAA1429 knockdown ($P < 0.01$, Figure 4D). RNA stability analysis showed that KIAA1429 analysis resulted in decreased stability of EBLN3P ($P < 0.01$, Figure 4E). EBLN3P was reduced after KIAA1429 knockdown ($P < 0.01$, Figure 4F). Collectively, KIAA1429 enhances LncRNA EBLN3P expression in an m6A-dependent manner.

Overexpression of EBLN3P inhibits ferroptosis to increase radioresistance in CRC cells

Next, we up-regulated EBLN3P expression in HCT116R cells ($P < 0.01$, Figure 5A) co-treated with si-KIAA1429-1. The ferroptosis level was reduced in cells overexpressing EBLN3P after 4 Gy radiation ($P < 0.05$, Figure 5B-E). The proliferation rate of cells increased after overexpression of EBLN3P ($P < 0.05$, Figure 5F), the number of clonal cells enhanced ($P < 0.01$, Figure 5G), and the positivity of γ-H2AX was markedly reduced ($P < 0.05$, Figure 5H). Altogether, overexpression of EBLN3P inhibited ferroptosis to increase radioresistance in CRC cells.

LncRNA EBLN3P competitively binds to miR-153-3p through the ceRNA network to promote KIAA1429 expression

In radioresistant cells, subcellular analysis revealed that EBLN3P was predominantly located in the cytoplasm (Figure 6A), which was consistent with the prediction of an online database (http://www.csbio.sjtu.edu.cn/bioinf/lncLocator/?tdsourcetag=s_pcqq_aiomsg) (Figure 6B). Thus, we analyzed the mechanism of EBLN3P-mediated ceRNA. We identified the miRNA between EBLN3P and KIAA1429 as miR-153-3p by taking the intersection (Figure 6C). Luciferase assay showed that miR-153-3p was closely associated with EBLN3P ($P < 0.01$, Figure 6D). Ago2-RIP experiments showed that miR-153-3p interacted with EBLN3P at the molecular level ($P < 0.01$, Figure 6E). miR-153-3p was closely associated with KIAA1429 mRNA 3'-UTR ($P < 0.01$, Figure 6F). miR-153-3p expression was reduced in CRC cells ($P < 0.01$, Figure 6G). EBLN3P downregulation promoted miR-153-3p expression and inhibited KIAA1429 expression ($P < 0.01$, Figure 6H-I), whereas overexpression of miR-153-3p also inhibited KIAA1429 expression ($P < 0.01$, Figure 6J-K). Taken together, lncRNA EBLN3P competitively binds to miR-153-3p through the ceRNA network to promote KIAA1429 expression.

Downregulation of miR-153-3p represses ferroptosis to increase radioresistance in CRC cells

Finally, we decreased miR-153-3p expression in HCT116R cells ($P < 0.01$, Figure 7A) co-treated with si-KIAA1429-1. After 4 Gy radiation, miR-153-3p downregulation resulted in decreased ferroptosis in the cells ($P < 0.05$, Figure 7B-E), increased proliferation ($P < 0.05$, Figure 7F), more clonal cells ($P < 0.01$, Figure 7G), and significantly decreased positivity of γ-H2AX ($P < 0.05$, Figure 7H). In short, miR-153-3p downregulation inhibited ferroptosis to increase radioresistance in CRC cells.

DISCUSSION

Radiotherapy is frequently used for treating CRC, and yet tumor resistance to radiotherapy is a major challenge [26]. After radiotherapy, cancer cells exhibit morphological alterations of mitochondria typical of ferroptosis and ferroptosis agonists can enhance the radiation efficacy of tumor models [27, 28]. KIAA1429 is associated with ferroptosis of multiple cancer cells except CRC [12, 29]. This article probed into the action of KIAA1429 on CRC cell ferroptosis and then radioresistance as well as the underlying mechanism of action. Our findings unveiled that KIAA1429-mediated m6A modification up-regulated LncRNA EBLN3P expression, and LncRNA EBLN3P in turn increased KIAA1429 expression by competitively binding to miR-153-3p, thus reducing ferroptosis and increasing the radioresistance of CRC.

KIAA1429 exhibits significantly high expression in CRC tissues, while CRC patients with higher expression of KIAA1429 have shorter overall survival than those with lower expression [30]. Our results displayed the same high expression of KIAA1429 in CRC cells. Moreover, our data revealed that CRC cells with KIAA1429 downregulation grew slower and had fewer number of clone cells. Also, the positive rate of γ-H2AX, a predictive tool in radiation oncology [31], was elevated in CRC cells after KIAA1429 knockdown. These results reflected that KIAA1429 could enhance the radiotherapy resistance of CRC cells. Consistently, in lung adenocarcinoma, KIAA1429 promotes cancer cell resistance to gefitinib and accelerates tumorigenesis [32]. Ferroptosis is an iron-dependent form of regulated cell death driven by an overload of lipid peroxides on cellular membranes [33]. SLC7A11, ROS, GSH, GPX4, Fe^{2+}, and ACSL4 are factors involved in ferroptosis manipulation [34]. Our results manifested that the levels of ACSL4 and ROS were augmented and the levels of SLC7A11, GPX4, and GSH were diminished in HCT116R and SW620R cells after silencing KIAA1429, suggesting that KIAA1429 downregulation strengthened ferroptosis of CRC cells. Certain cancer cells with acquired drug resistance have been shown to exert antitumor effects by inducing ferroptosis

[35]. Similarly, our results demonstrated that ferroptosis inhibition mediated by Fer-1 contributed to CRC cell proliferation, colony growth, and γ-H2AX positive rate reduction. Collectively, KIAA1429 could enhance CRC cell radioresistance through ferroptosis suppression.

Researchers have identified that KIAA1429 regulates lncRNA POU6F2-AS1 to aggravate CRC progression in an m6A modification manner [36]. LncRNA EBLN3P displays a significant elevation in CRC patients [16], which was consistent with our results. Moreover, we found m6A sites on the EBLN3P sequence and that m6A enrichment declined in CRC cells with silenced KIAA1429. Furthermore, KIAA1429 downregulation led to lower EBLN3P stability and expression levels. Thus, it could be inferred that KIAA1429 could stimulate EBLN3P expression in an m6A-dependent manner. In non-small cell lung cancer cells, EBLN3P can enhance ROS production, which plays a crucial role in regulating radioresistance [37]. We, therefore, analyzed whether EBLN3P had any effects on CRC cell ferroptosis and radioresistance. Interestingly, following EBLN3P upregulation, CRC cells exhibited suppressed ferroptosis and experienced rapid proliferation, colony formation, and increased γ-H2AX positive rate. Higher EBLN3P was associated with methotrexate resistance, and the downregulation of EBLN3P decreased the methotrexate resistance of osteosarcoma cells [38]. The expression of EBLN3P was higher in lung cancer tissues and reduced by carbon ion irradiation [39]. There is no report about the regulation of lncRNA EBLN3P in ferroptosis and radioresistance in CRC. Hence, our present study first highlights that lncRNA EBLN3P could enhance the radioresistance of CRC cells by suppressing ferroptosis.

LncRNA-miRNA interaction is involved in CRC pathogenesis [40]. LncRNA EBLN3P regulates UHMK1 expression by sponging miR-323a-3p and contributes to CRC development [16]. miR-153 promotes cellular invasion in the progression of CRC and miR-153-3p interaction with SNHG17-COL11A1/IGFBP3/KLF6 or with TUG1-

DAPK1/ARNT2/KLK3/PLD1/SMAD2 might involve in early-stage colon adenocarcinoma [41]. In CRC patients, miR-153-5p negatively correlates with LINC00511 [42]. Our results suggested that miR-153-3p was poorly expressed in CRC cells and EBLN3P downregulation elevated miR-153-3p expression while suppressing KIAA1429 expression. That was to say, lncRNA EBLN3P could increase KIAA1429 expression by competitively binding to miR-153-3p through the ceRNA network. There is rare research about the role of miR-153-3p in ferroptosis. Only one previous study elicited miR-153 engagement in breast cancer ferroptosis [43]. What's more, miR-153-3p can enhance cell radiosensitivity in human glioma by targeting BCL2 [44]. Our results further evinced that miR-153-3p downregulation could increase the radioresistance of CRC cells by hindering ferroptosis.

CONCLUSION

In summary, our results show that KIAA1429-mediated m6A modification upregulates lncRNA EBLN3P, whereas lncRNA EBLN3P elevates KIAA1429 expression by competitively binding to miR-153-3p through the ceRNA network, thus lowering the ferroptosis level and enhancing radioresistance of CRC cells. Several limitations should be addressed in our future studies, though. First, the proposed mechanism of action was verified at the cellular level only and we lacked animal experiments to further verify the findings, and clinical application was far away. Second, there are plenty of molecular mechanisms downstream of KIAA1429 that await exploration; the ceRNA mechanism of EBLN3P in radioresistance remained insufficiently investigated. Finally, whether there are other target genes downstream of miR-153-3p remained a mystery to us, which needs to be uncovered and validated by further experimentation. In the future, the verification of the above functional mechanism in animal models and the downstream mechanism of miR-153-3p are topics worthy of further research to shed light on the better management of CRC.

Data availability

The datasets supporting the conclusions of this article are presented in the article. Further inquiries can be directed to the corresponding author.

REFERENCES

1. Shin AE, Giancotti FG, Rustgi AK. Metastatic colorectal cancer: mechanisms and emerging therapeutics. Trends Pharmacol Sci 2023;44(4):222-36. https://doi.org/10.1016/j.tips.2023.01.003.

2. Siegel RL, Wagle NS, Cercek A, Smith RA, Jemal A. Colorectal cancer statistics, 2023. CA Cancer J Clin 2023;73(3):233-54. https://doi.org/10.3322/caac.21772.

3. Ionescu VA, Gheorghe G, Bacalbasa N, Chiotoroiu AL, Diaconu C. Colorectal Cancer: From Risk Factors to Oncogenesis. Medicina (Kaunas) 2023;59(9). https://doi.org/10.3390/medicina59091646.

4. Wang QQ, Zhou YC, Zhou Ge YJ, Qin G, Yin TF, Zhao DY, et al. Comprehensive proteomic signature and identification of CDKN2A as a promising prognostic biomarker and therapeutic target of colorectal cancer. World J Clin Cases 2022;10(22):7686-97. https://doi.org/10.12998/wjcc.v10.i22.7686.

5. Zhao H, Ming T, Tang S, Ren S, Yang H, Liu M, et al. Wnt signaling in colorectal cancer: pathogenic role and therapeutic target. Mol Cancer 2022;21(1):144. https://doi.org/10.1186/s12943-022-01616-7.

6. Weng J, Li S, Zhu Z, Liu Q, Zhang R, Yang Y, et al. Exploring immunotherapy in colorectal cancer. J Hematol Oncol 2022;15(1):95. https://doi.org/10.1186/s13045-022-01294-4.

7. Ciardiello F, Ciardiello D, Martini G, Napolitano S, Tabernero J, Cervantes A. Clinical management of metastatic colorectal cancer in the era of precision medicine. CA Cancer J Clin 2022;72(4):372-401. https://doi.org/10.3322/caac.21728.

8. Chen XY, Zhang J, Zhu JS. The role of m(6)A RNA methylation in human cancer. Mol Cancer 2019;18(1):103. https://doi.org/10.1186/s12943-019-1033-z.

9. Zhang X, Li MJ, Xia L, Zhang H. The biological function of m6A methyltransferase KIAA1429 and its role in human disease. PeerJ 2022;10(e14334. https://doi.org/10.7717/peerj.14334.

10. Huang J, Shao Y, Gu W. Function and clinical significance of N6-methyladenosine in digestive system tumours. Exp Hematol Oncol 2021;10(1):40. https://doi.org/10.1186/s40164-021-00234-1.

11. Li Y, He L, Wang Y, Tan Y, Zhang F. N(6)-methyladenosine methyltransferase KIAA1429 elevates colorectal cancer aerobic glycolysis via HK2-dependent manner. Bioengineered 2022;13(5):11923-32. https://doi.org/10.1080/21655979.2022.2065952.

12. Xu K, Dai X, Yue J. m(6)A methyltransferase KIAA1429 accelerates oral squamous cell carcinoma via regulating glycolysis and ferroptosis. Transl Oncol 2023;36(101745. https://doi.org/10.1016/j.tranon.2023.101745.

13. Wu Y, Song Y, Wang R, Wang T. Molecular mechanisms of tumor resistance to radiotherapy. Mol Cancer 2023;22(1):96. https://doi.org/10.1186/s12943-023-01801-2.

14. Bridges MC, Daulagala AC, Kourtidis A. LNCcation: lncRNA localization and function. J Cell Biol 2021;220(2). https://doi.org/10.1083/jcb.202009045.

15. Javed Z, Khan K, Sadia H, Raza S, Salehi B, Sharifi-Rad J, et al. LncRNA & Wnt signaling in colorectal cancer. Cancer Cell Int 2020;20(326. https://doi.org/10.1186/s12935-020-01412-7.

16. Xu XH, Song W, Li JH, Huang ZQ, Liu YF, Bao Q, et al. Long Non-coding RNA EBLN3P Regulates UHMK1 Expression by Sponging miR-323a-3p and Promotes Colorectal Cancer Progression. Front Med (Lausanne) 2021;8(651600. https://doi.org/10.3389/fmed.2021.651600.

17. Wang L, Cho KB, Li Y, Tao G, Xie Z, Guo B. Long Noncoding RNA (lncRNA)-Mediated Competing Endogenous RNA Networks Provide Novel Potential Biomarkers and

Therapeutic Targets for Colorectal Cancer. Int J Mol Sci 2019;20(22). https://doi.org/10.3390/ijms20225758.

18. Hussen BM, Hidayat HJ, Salihi A, Sabir DK, Taheri M, Ghafouri-Fard S. MicroRNA: A signature for cancer progression. Biomed Pharmacother 2021;138(111528. https://doi.org/10.1016/j.biopha.2021.111528.

19. Gu J, Sun R, Tang D, Liu F, Chang X, Wang Q. Astragalus mongholicus Bunge-Curcuma aromatica Salisb. suppresses growth and metastasis of colorectal cancer cells by inhibiting M2 macrophage polarization via a Sp1/ZFAS1/miR-153-3p/CCR5 regulatory axis. Cell Biol Toxicol 2022;38(4):679-97. https://doi.org/10.1007/s10565-021-09679-w.

20. Lin Y, Shi H, Wu L, Ge L, Ma Z. Research progress of N6-methyladenosine in colorectal cancer: A review. Medicine (Baltimore) 2023;102(47):e36394. https://doi.org/10.1097/MD.0000000000036394.

21. Shang Y, Wang L, Zhu Z, Gao W, Li D, Zhou Z, et al. Downregulation of miR-423-5p Contributes to the Radioresistance in Colorectal Cancer Cells. Front Oncol 2020;10(582239. https://doi.org/10.3389/fonc.2020.582239.

22. Agarwal V, Bell GW, Nam JW, Bartel DP. Predicting effective microRNA target sites in mammalian mRNAs. Elife 2015;4(https://doi.org/10.7554/eLife.05005.

23. Li JH, Liu S, Zhou H, Qu LH, Yang JH. starBase v2.0: decoding miRNA-ceRNA, miRNA-ncRNA and protein-RNA interaction networks from large-scale CLIP-Seq data. Nucleic Acids Res 2014;42(Database issue):D92-7. https://doi.org/10.1093/nar/gkt1248.

24. Ren S, Zhang Y, Yang X, Li X, Zheng Y, Liu Y, et al. N6-methyladenine- induced LINC00667 promoted breast cancer progression through m6A/KIAA1429 positive feedback loop. Bioengineered 2022;13(5):13462-73. https://doi.org/10.1080/21655979.2022.2077893.

25. Livak KJ, Schmittgen TD. Analysis of relative gene expression data using real-time quantitative PCR and the 2(-Delta Delta C(T)) Method. Methods 2001;25(4):402-8. https://doi.org/10.1006/meth.2001.1262.

26. Wang C, Yuan M, Gao Y, Hou R, Song D, Feng Y. Changes in Tumor Immune Microenvironment after Radiotherapy Resistance in Colorectal Cancer: A Narrative Review. Oncol Res Treat 2023;46(5):177-91. https://doi.org/10.1159/000530161.

27. Lu Z, Xiao B, Chen W, Tang T, Zhuo Q, Chen X. The potential of ferroptosis combined with radiotherapy in cancer treatment. Front Oncol 2023;13(1085581. https://doi.org/10.3389/fonc.2023.1085581.

28. Beretta GL, Zaffaroni N. Radiotherapy-induced ferroptosis for cancer treatment. Front Mol Biosci 2023;10(1216733. https://doi.org/10.3389/fmolb.2023.1216733.

29. Wu Y, Li H, Huang Y, Chen Q. Silencing of m(6)A methyltransferase KIAA1429 suppresses the progression of non-small cell lung cancer by promoting the p53 signaling pathway and ferroptosis. Am J Cancer Res 2023;13(11):5320-33.

30. Ma L, Lin Y, Sun SW, Xu J, Yu T, Chen WL, et al. KIAA1429 is a potential prognostic marker in colorectal cancer by promoting the proliferation via downregulating WEE1 expression in an m6A-independent manner. Oncogene 2022;41(5):692-703. https://doi.org/10.1038/s41388-021-02066-z.

31. Pouliliou S, Koukourakis MI. Gamma histone 2AX (gamma-H2AX)as a predictive tool in radiation oncology. Biomarkers 2014;19(3):167-80. https://doi.org/10.3109/1354750X.2014.898099.

32. Lin X, Ye R, Li Z, Zhang B, Huang Y, Du J, et al. KIAA1429 promotes tumorigenesis and gefitinib resistance in lung adenocarcinoma by activating the JNK/ MAPK pathway in an m(6)A-dependent manner. Drug Resist Updat 2023;66(100908. https://doi.org/10.1016/j.drup.2022.100908.

33. Lei G, Zhuang L, Gan B. Targeting ferroptosis as a vulnerability in cancer. Nat Rev Cancer 2022;22(7):381-96. https://doi.org/10.1038/s41568-022-00459-0.

34. Wang Y, Zhang Z, Sun W, Zhang J, Xu Q, Zhou X, et al. Ferroptosis in colorectal cancer: Potential mechanisms and effective therapeutic targets. Biomed Pharmacother 2022;153(113524. https://doi.org/10.1016/j.biopha.2022.113524.

35. Tong X, Tang R, Xiao M, Xu J, Wang W, Zhang B, et al. Targeting cell death pathways for cancer therapy: recent developments in necroptosis, pyroptosis, ferroptosis, and cuproptosis research. J Hematol Oncol 2022;15(1):174. https://doi.org/10.1186/s13045-022-01392-3.

36. Lu D, Chen A. lncRNA POU6F2-AS1 Regulated by KIAA1429 Contributes to Colorectal Cancer Progression in an m(6)A Modification Manner. Mol Biotechnol 2023. https://doi.org/10.1007/s12033-023-00986-7.

37. Tang H, Liu S, Yan X, Jin Y, He X, Huang H, et al. Inhibition of LNC EBLN3P Enhances Radiation-Induced Mitochondrial Damage in Lung Cancer Cells by Targeting the Keap1/Nrf2/HO-1 Axis. Biology (Basel) 2023;12(9). https://doi.org/10.3390/biology12091208.

38. Sun MX, An HY, Sun YB, Sun YB, Bai B. LncRNA EBLN3P attributes methotrexate resistance in osteosarcoma cells through miR-200a-3p/O-GlcNAc transferase pathway. J Orthop Surg Res 2022;17(1):557. https://doi.org/10.1186/s13018-022-03449-y.

39. Tang H, Huang H, Guo Z, Huang H, Niu Z, Ji Y, et al. Heavy Ion-Responsive lncRNA EBLN3P Functions in the Radiosensitization of Non-Small Cell Lung Cancer Cells Mediated by TNPO1. Cancers (Basel) 2023;15(2). https://doi.org/10.3390/cancers15020511.

40. Alshahrani SH, Al-Hadeithi ZSM, Almalki SG, Malviya J, Hjazi A, Mustafa YF, et al. LncRNA-miRNA interaction is involved in colorectal cancer pathogenesis by modulating diverse signaling pathways. Pathol Res Pract 2023;251(154898. https://doi.org/10.1016/j.prp.2023.154898.

41. Liu JX, Li W, Li JT, Liu F, Zhou L. Screening key long non-coding RNAs in early-stage colon adenocarcinoma by RNA-sequencing. Epigenomics 2018;10(9):1215-28. https://doi.org/10.2217/epi-2017-0155.

42. Sun S, Xia C, Xu Y. HIF-1alpha induced lncRNA LINC00511 accelerates the colorectal cancer proliferation through positive feedback loop. Biomed Pharmacother 2020;125(110014. https://doi.org/10.1016/j.biopha.2020.110014.

43. Huang X, Wu J, Wang Y, Xian Z, Li J, Qiu N, et al. FOXQ1 inhibits breast cancer ferroptosis and progression via the circ_0000643/miR-153/SLC7A11 axis. Exp Cell Res 2023;431(1):113737. https://doi.org/10.1016/j.yexcr.2023.113737.

44. Sun D, Mu Y, Piao H. MicroRNA-153-3p enhances cell radiosensitivity by targeting BCL2 in human glioma. Biol Res 2018;51(1):56. https://doi.org/10.1186/s40659-018-0203-6.

TABLES AND FIGURES WITH LEGENDS

TABLE 1. PCR primer sequences

Name	Sequence (5'-3')
KIAA1429	F: CGAGCGCTGAGCAAAGTTCT
	R: TGGGGGTATGACTCGGACTT
LncRNA EBLN3P	F: GTCCAGTCTTTGAGGACCGA
	R: CCTATGCCCAGATCGTCCAA
GAPDH	F: GTCAAGGCTGAGAACGGGAA
	R: TCGCCCCACTTGATTTTGGA
miR-153-3p	F: GCGTCGATTGCATAGTCACAA
	R: AACTGGTGTCGTGGAGTCGG
U6	F: TCGCTTCGGCAGCACATATACT
	R: GCTTCACGAATTTGCGTGTCATC

PCR: Polymerase chain reaction; KIAA1429: Vir like m6A methyltransferase associated; LncRNA EBLN3P：endogenous Bornavirus like nucleoprotein 3, pseudogene；GAPDH：glyceraldehyde-3-phosphate dehydrogenase

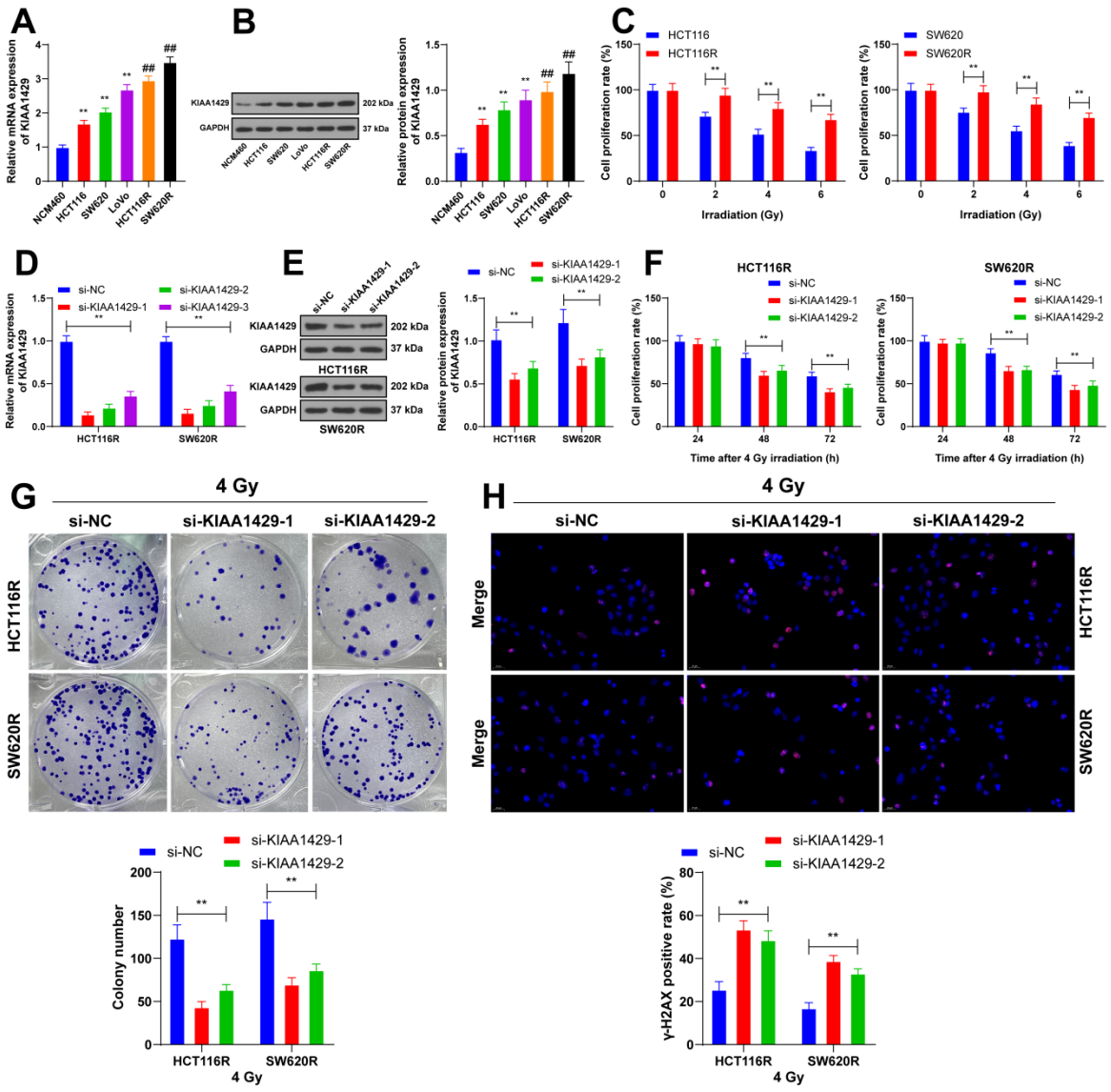

FIGURE 1. KIAA1429 increases radioresistance in CRC cells. (A-B) RT-qPCR and western blot to detect the expression of KIAA1429 in cells, ** $P < 0.01$, compared with NCM460, ## $P < 0.01$ compared with parental cells; (C) Radioresistant cell lines were constructed and the proliferation rate of cells was detected by CCK-8 assay at different doses of radiation for 48 h; si- KIAA1429 was transfected into radioresistant cells, and si-NC was used as a control. (D-E) the expression of KIAA1429 in the cells was detected by RT-qPCR and western blot; (F) CCK-8 to detect the proliferation rate of cells after different times of 4 Gy of radiation; (G) Colony formation assay to detect the cloning ability of the cells after 4 Gy of radiation; (H) Immunofluorescence to detect the positive rate of γ-H2AX in cells after 48 h of 4 Gy radiation. Three independent replicate tests were performed, and the data were expressed as mean ± standard deviation; one-way ANOVA was used for data comparisons among multiple groups in panels AB, two-way ANOVA was used for data comparisons among multiple groups in panels C-H, and Tukey's multiple comparisons test was used for all post-hoc tests. ** $P < 0.01$. RT-

qPCR: Reverse transcription-quantitative polymerase chain reaction; CCK-8: Cell Counting Kit-8; γ-H2AX: Histone H2AX; si-KIAA1429: KIAA1429 siRNA; si-NC: NC siRNA; ANOVA: Analysis of variance.

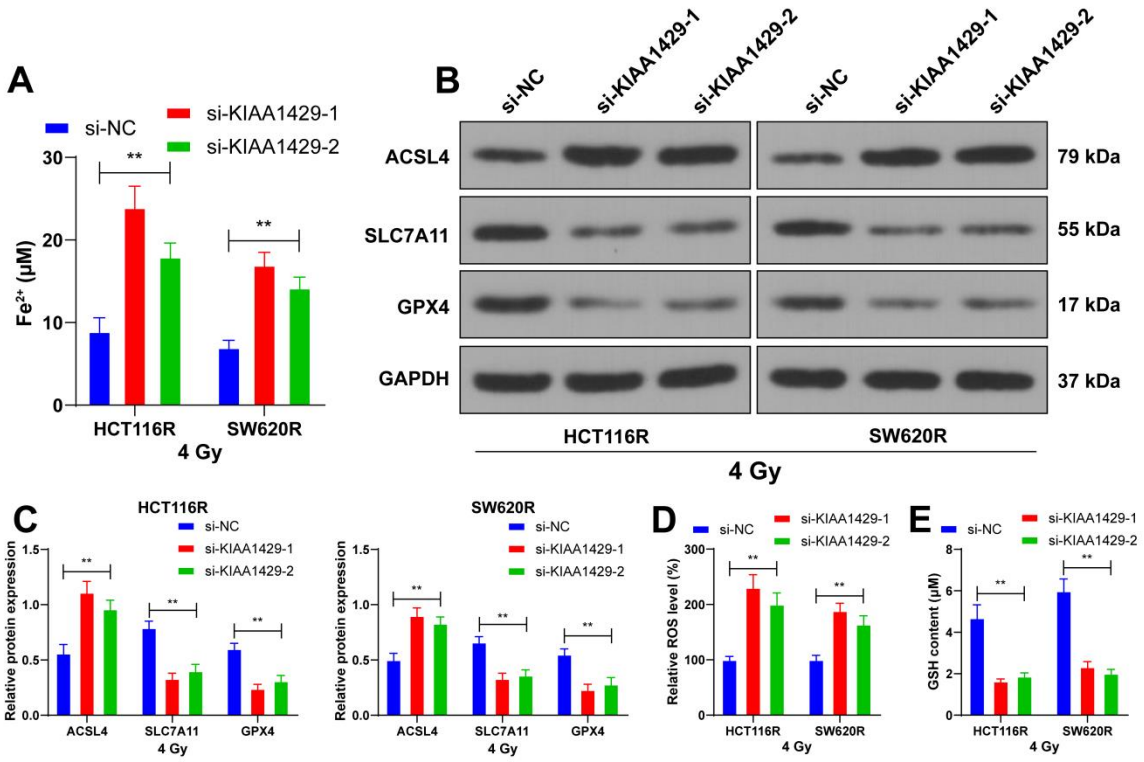

FIGURE 2. KIAA1429 knockdown promotes ferroptosis in CRC cells. The si-KIAA1429 was transfected into radioresistant cells, and si-NC was used as a control. (A) 48 h after 4 Gy radiation, the level of Fe^{2+} in cells with different transfections was detected; (B-C) the expression of ferroptosis-related proteins ACSL4, SLC7A11, and GPX4 in cells with different transfections was detected by Western blot; (D) the level of ROS in cells with different transfections; (E) the cellular changes in GSH levels in cells with different transfections. Three independent replicate assays were performed, and the data were expressed as mean ± standard deviation. Comparison of data among multiple groups was performed by two-way ANOVA, and Tukey's test was used for all post hoc tests. ** $P < 0.01$. si-KIAA1429: KIAA1429 siRNA; si-NC: NC siRNA; ACSL4: Acyl Coenzyme A Synthetase Long Chain 4; GPX4: Glutathione peroxidase 4; SLC7A11: Solute carrier family 7-member 11; ROS: Reactive oxygen species; GSH: Glutathione; ANOVA: Analysis of variance.

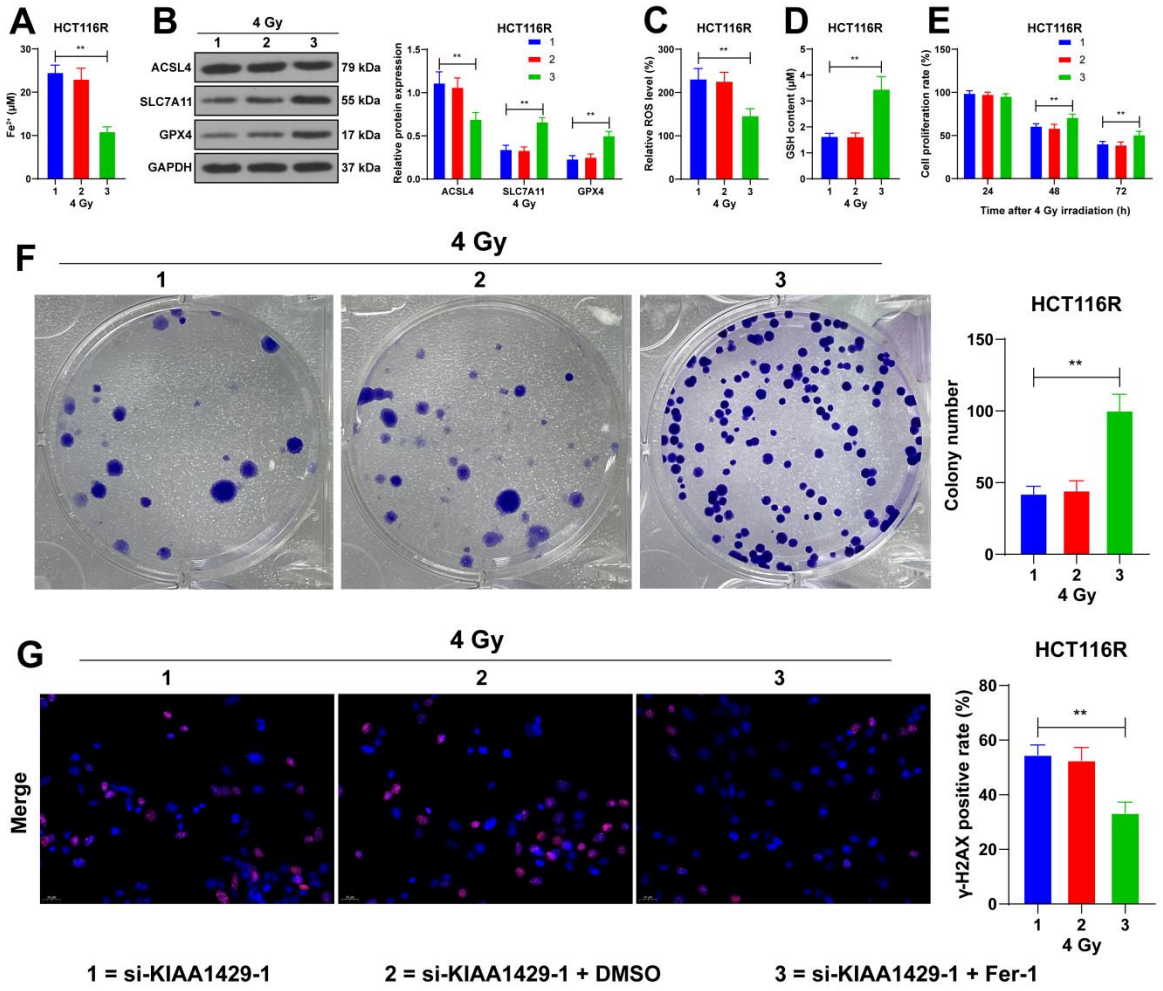

FIGURE 3. KIAA1429 increases radioresistance in CRC cells by inhibiting ferroptosis. HCT116R cells were treated with Ferrostatin-1 (Fer-1), and DMSO treatment was used as a control. (A) after 48 h of 4 Gy radiation, the level of Fe^{2+} in cells in cells with different treatments was detected; (B) the expression of ferroptosis-related proteins ACSL4, SLC7A11, and GPX4 in the cells with different treatments was detected by Western blot; (C) the level of ROS in cells with different treatments; (D) Changes of GSH content in cells with different treatments; (E) CCK-8 to detect the proliferation rate of cells after different time of 4 Gy radiation; (F) Colone formation assay to detect the cloning ability of cells after 4 Gy radiation; (G) Immunofluorescence to detect the positive rate of γ-H2AX in cells after 48 h of 4 Gy radiation. Three independent replicate tests were performed, and the data were expressed as mean ± standard deviation; one-way ANOVA was used to compare the data among multiple groups in panels ACDFG, two-way ANOVA was used to compare the data among multiple groups in panels BE, and Tukey's test was used in all post-hoc tests. ** $P < 0.01$. Fer-1: Ferrostatin-1; si-KIAA1429: KIAA1429 siRNA; ACSL4: Acyl Coenzyme A Synthetase Long Chain 4; GPX4: Glutathione peroxidase 4; SLC7A11: Solute carrier family 7-member 11; ROS: Reactive oxygen species; GSH: Glutathione; CCK-8: Cell Counting Kit-8; γ-H2AX: Histone H2AX; ANOVA: Analysis of variance.

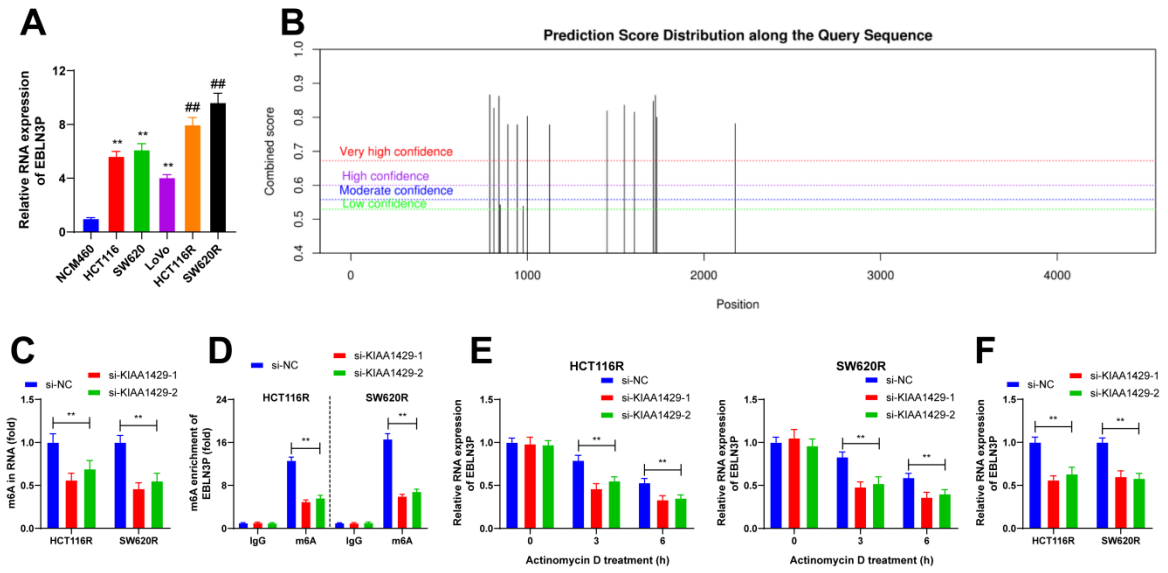

FIGURE 4. KIAA1429-mediated m6A modification upregulates the expression of LncRNA EBLN3P. (A) RT-qPCR detection of EBLN3P expression in cells of each group, ** $P < 0.01$ compared with NCM460, ## $P < 0.01$ compared with parental cells; (B) m6A online tool predicts m6A modification sites of EBLN3P; (C) m6A quantification to analyze m6A enrichment in cells with different transfections; (D) MeRIP analyzes the m6A level in EBLN3P RNA in cells with different transfections; (E) RT-qPCR to detect the RNA stability of EBLN3P in cells with different transfections; (F) RT-qPCR to detect EBLN3P expression in cells with different transfections. Three independent replicate assays were performed, and the data were expressed as mean ± standard deviation; one-way ANOVA was used to compare the data among multiple groups in panel A, two-way ANOVA was used to compare the data among multiple groups in panels B-F, and Tukey's test was used in all post-hoc tests. ** $P < 0.01$. RT-qPCR: reverse transcription-quantitative polymerase chain reaction; m6A: N6-methyladenosine; MeRIP: RNA methylation immunoprecipitation; si-KIAA1429：KIAA1429 siRNA; si-NC: NC siRNA; ANOVA: analysis of variance.

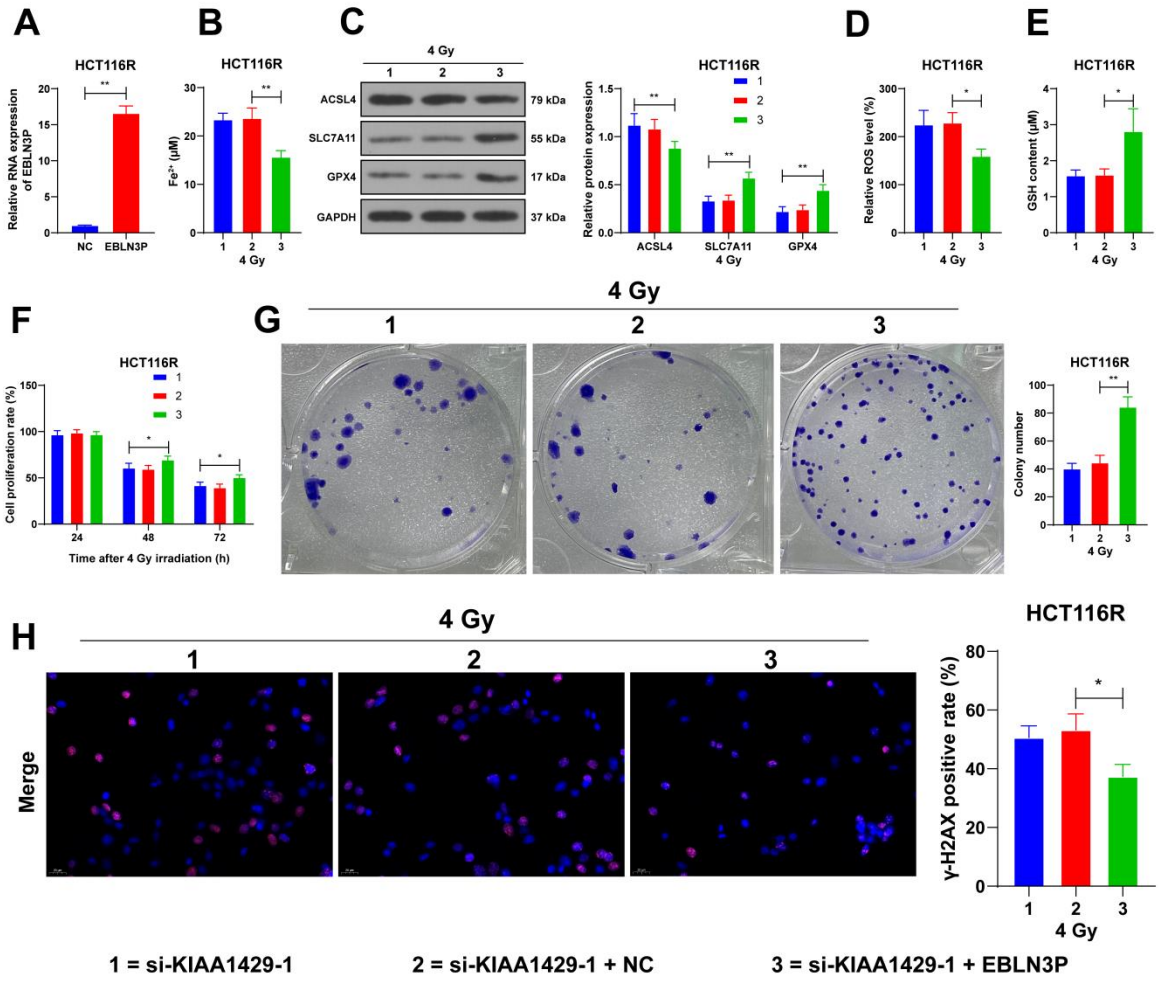

FIGURE 5. Overexpression of EBLN3P inhibits ferroptosis to increase radioresistance in CRC cells. HCT116R cells were treated with Ferrostatin-1 (Fer-1), and DMSO treatment was used as a control. (A) after 48 h of 4 Gy radiation, EBLN3P expression in cells detected by RT-qPCR; (B) the level of Fe^{2+} in cells after overexpression of EBLN3P was detected; (C) the expression of ferroptosis-related proteins ACSL4, SLC7A11, and GPX4 was detected in cells after overexpression of EBLN3P by Western blot; (D) the level of ROS; (E) Changes of GSH content in cells after overexpression of EBLN3P; (F) CCK-8 to detect the proliferation rate of cells after different time of 4 Gy radiation; (G) Colone formation assay to detect the cloning ability of cells after 4 Gy radiation; (H) Immunofluorescence to detect the positive rate of γ-H2AX in cells after 48 h of 4 Gy radiation. Three independent replicate tests were performed, and the data were expressed as mean ± standard deviation; the t test was used to compare the data in panel A, one-way ANOVA was used to compare the data among multiple groups in panels BDEFG, two-way ANOVA was used to compare the data among multiple groups in panel C, and Tukey's test was used in all post-hoc tests. *$P < 0.05$, ** $P < 0.01$. EBLN3P: EBLN3P overexpression vectors; NC: Empty vector; RT-qPCR: Reverse transcription-quantitative polymerase chain reaction; ACSL4: Acyl coenzyme a synthetase long chain 4; GPX4:

Glutathione peroxidase 4; SLC7A11: Solute carrier family 7-member 11; ROS: Reactive oxygen species; GSH: Glutathione; CCK-8: Cell Counting Kit-8; γ-H2AX: Histone H2AX; ANOVA: Analysis of variance.

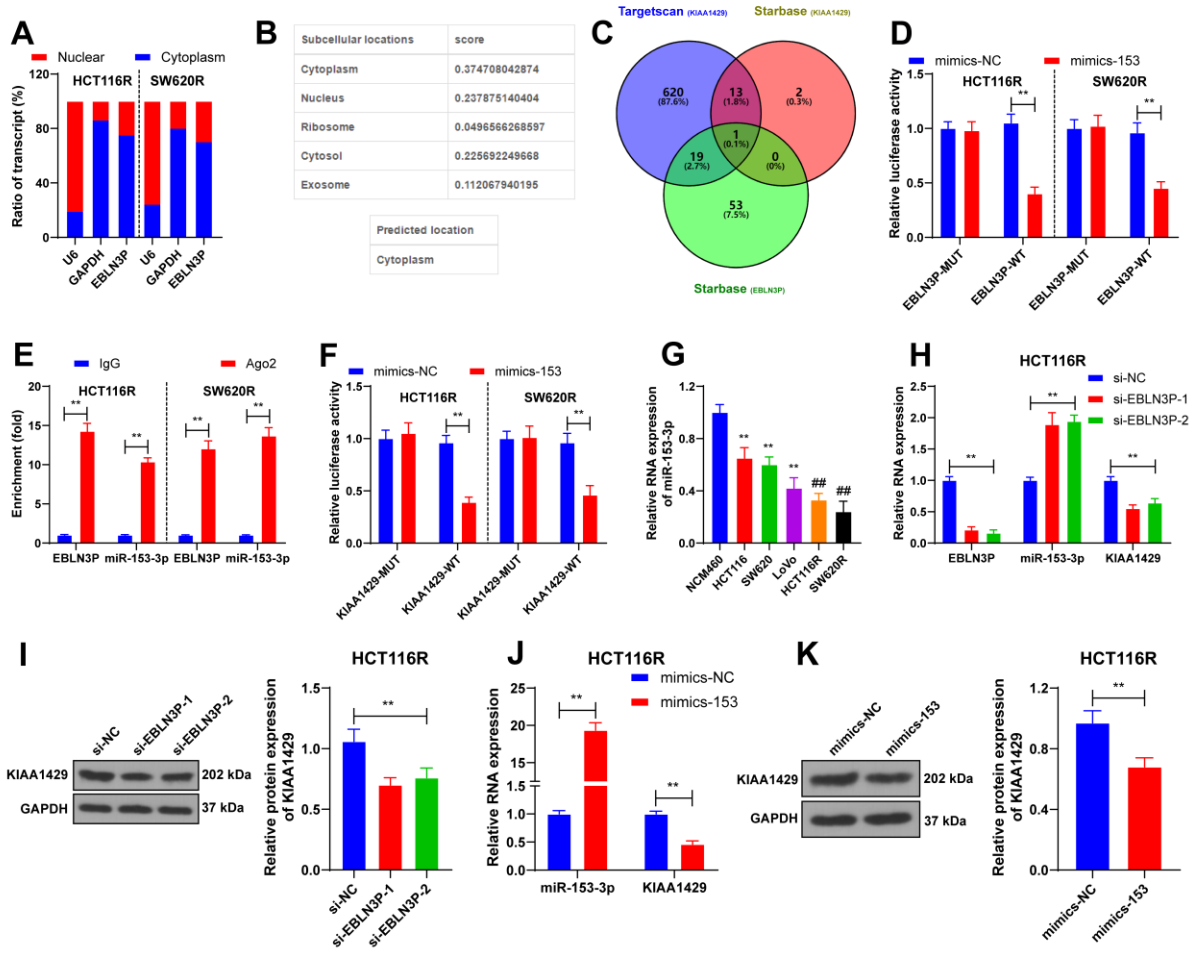

FIGURE 6. LncRNA EBLN3P competitively binds to miR-153-3p through the ceRNA network to promote KIAA1429 expression. (A) Nuclear/cytoplasmic fractionation to detect the subcellular localization of EBLN3P in CRC cells; (B) Database prediction of the subcellular localization of EBLN3P; (C) Targetscan and Starbase databases to predict the ceRNA mechanism of EBLN3P; (D-F) Dual-luciferase and RIP experiments to validate the ceRNA mechanism of EBLN3P in CRC cells; (G) RT-qPCR to detect the expression of miR-153-3p in cells of each group, ** $P < 0.01$ compared with NCM460, ## $P < 0.01$ compared with parental cells; (H) RT-qPCR to detect the expression of EBLN3P, miR-153-3p, and KIAA1429 after transfection of si-EBLN3P; (I) Western blot to detect the expression of KIAA1429 after transfection of si-EBLN3P; (J) RT-qPCR to detect the expression of miR-153-3p and KIAA1429 after transfection of mimics-153; (K) western blot to detect the expression of KIAA1429 after transfection of mimics-153. Three independent replicate assays were performed, and the data were expressed as mean ± standard deviation; t-test was used to compare the data between the two groups in panel K; one-way ANOVA was used to compare the data among multiple groups in panels G/I, two-way ANOVA was used to compare the data among multiple groups in panels DEFHJ, and Tukey's test was used in all post-hoc tests. ** $P < 0.01$. RIP: RNA immunoprecipitation; ceRNA: Competing endogenous RNA; RT-qPCR: Rreverse transcription-quantitative polymerase chain

reaction; si-EBLN3P: LncRNA EBLN3P siRNA; si-NC: NC siRNA; mimics-153: miR-153-3p mimics; mimics-NC: NC mimics; ANOVA: Analysis of variance.

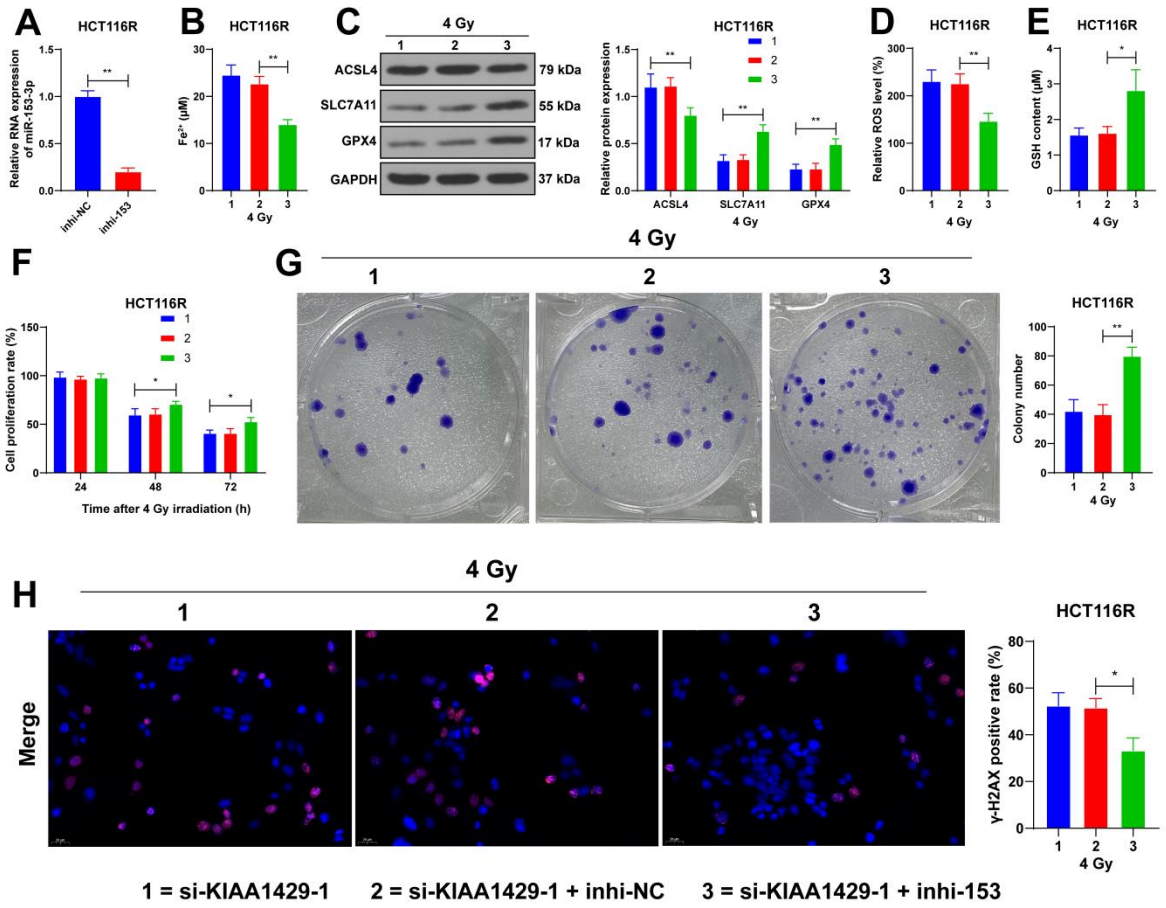

FIGURE 7. Downregulation of miR-153-3p represses ferroptosis to increase radioresistance in CRC cells. Inhi-153 was transfected into HCT116R cells, with inhi-NC as a control. (A) After 48 h of radiation at 4 Gy, the expression of miR-153-3p in cells was detected by RT-qPCR; (B) the level of Fe^{2+} in the cells after inhi-153 transfection; (C) Western blot to detect the expression of ferroptosis-related proteins ACSL4, SLC7A11, and GPX4; (D) ROS level in cells after inhi-153 transfection; (E) changes in GSH content in cells after inhi-153 transfection; (F) CCK-8 to detect the proliferation rate of cells after different times of 4 Gy radiation; (G) colony formation assay to detect the cloning ability of cells after 4 Gy radiation; (H) immunofluorescence to detect the positivity of γ-H2AX in cells after 48 h of 4 Gy radiation. Three independent replicate tests were performed, and the data were expressed as the mean ± standard deviation; t-test was used to compare the data between two groups in panel A; one-way ANOVA was used to compare the data among multiple groups in panels BDEGH, and two-way ANOVA was used to compare the data among multiple groups in panels CF, and the post hoc tests were used in all cases by Tukey's test.* $P < 0.05$, ** $P < 0.01$. inhi-153: miR-153-3p inhibitor; inhi-NC: NC inhibitor; RT-qPCR: Reverse transcription-quantitative polymerase chain reaction; ACSL4: Acyl Coenzyme A Synthetase Long Chain 4; GPX4: Glutathione peroxidase 4; SLC7A11: Solute carrier

family 7-member 11; ROS: Reactive oxygen species; GSH: Glutathione; CCK-8: Cell Counting Kit-8; γ-H2AX: Histone H2AX; ANOVA: Analysis of variance.

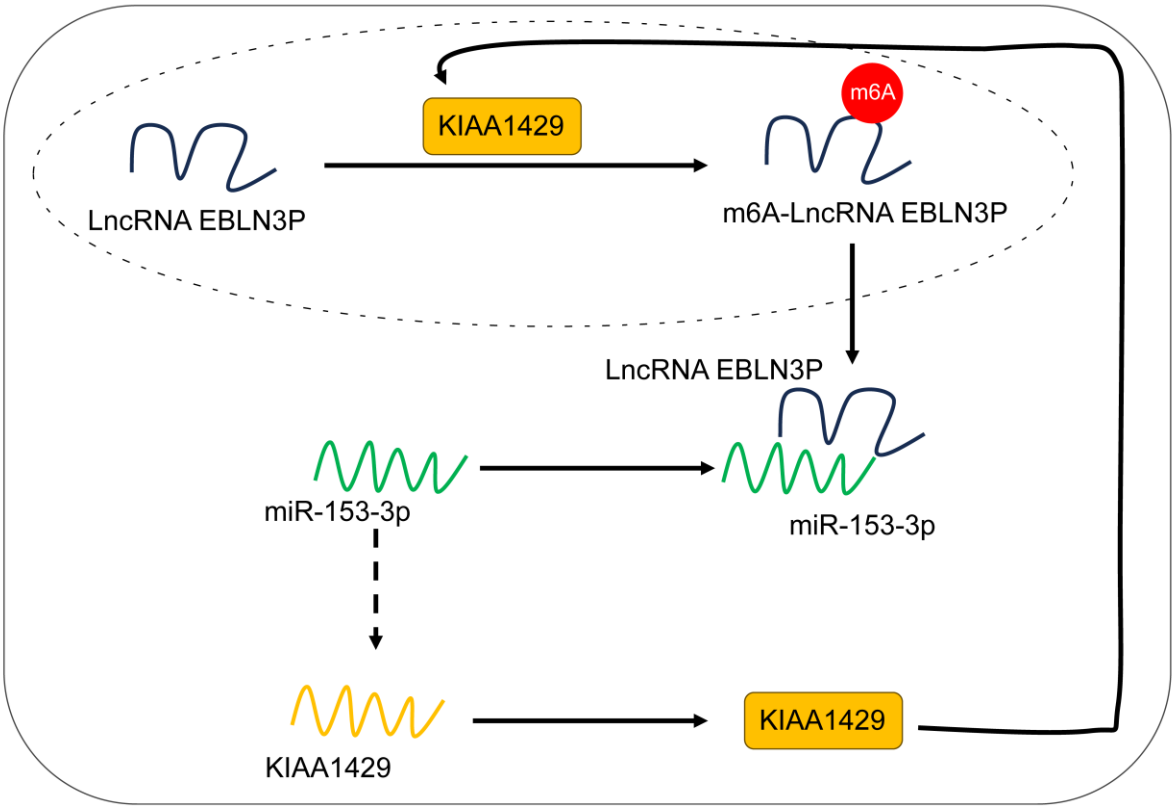

FIGURE 8. KIAA1429/LncRNA EBLN3P/miR-153-3p feedback loop increases radioresistance in colorectal cancer cells by decreasing ferroptosis.